Supplemental Table 1

	mRNA			Protein		
Tumor cell line	**MSLN (TPM)**	**HLA-A (TPM)**	**A*02:MSLN ratio**	**MSLN (#mol/cell)**	**A*02 (#mol/cell)**	**A*02:MSLN ratio**
MS751 (cervix; A*02:01, A*24:02)	205	156	0.4	12,000	28,000	2.3
MS751 (transduced with A*02)	205	438	2.1	12,000	301,000	25
HeLa (cervix; A*68:02, A*68:02; transduced with A*02)	66	85	na	27,000	740,000	27
OVCAR-3 (ovary; A*02:01, A*29:02)	70	81	0.6	51,000	25,000	0.5
U2OS (bone; A*02:01, A*32:01)	25	108	2.2	9,600	18,000	1.9
SW982 (synovium; A*02:01, A*02:01)	22	533	24	12,000	240,000	20
Tumor	**MSLN (TPM)**	**A*02 (TPM)**	**A*02:MSLN ratio**			
Lung adenocarcinoma	371	LOH	na			
Mesothelioma	784	LOH	na			
Ovarian	511	LOH	na			
Normal tissue (GTEx)	**MSLN (TPM)**	**HLA-A (TPM)**	**A*02:MSLN ratio**			
Lung	88	1934	22			

Supplemental Table 1. Summary of cell lines used in this study. Quantification of surface densities of MSLN and A*02 in various cancer cell lines, and corresponding reported mRNA levels in cell lines (CCLE) and normal lung tissue (GTEx). Surface MSLN and A*02 protein levels of engineered and wild-type tumor cell lines were quantified using QIFIKIT (quantitative analysis kit, Agilent). Where cell line HLA-A haplotypes are heterozygous for A*02, the TPM values were divided by 2. Note that in certain cases the HLA-A allele copy number is not known. The TPM value of MS751 + transduced A*02 (438 TPM) was estimated from measurement of its surface A*02 protein level using the standard curve in figure 2B. For HeLa cells, HLA-A (TPM) reports endogenous HLA-A levels (A*68) prior to transduction with A*02. Cell lines transduced with A*02 better mimic the A*02:MSLN ratio of normal lung tissue than cell lines expressing endogenous levels of the proteins (yellow boxes). We have not observed correlation between MSLN and HLA-A expression or deletion status. TPM, transcripts per million; na, not applicable.

Supplemental Table 2

	Cell line	Avg	Stan dev
1	OVCAR-3	51,000	12,000
2	HeLa	27,000	1,900
3	SW982	12,000	730
4	MS751	12,000	1,700
5	U2OS	9,600	2,800
6	SW480	2,200	1,200
7	HEPG2	1,900	120
8	H508	1,000	400
9	LnCAP clone FGC	930	220
10	A498	820	39
11	A375	630	170
12	Raji	180	5
13	SHP77	180	-
14	K562	n/a	n/a

Supplemental Table 2. Quantification of MSLN molecules/cell using QIFIKIT. Anti-human MSLN mouse antibody clone 618923 (R&D Systems) was used to stain 100,000 cells. After washing the cells, anti-mouse IgG F(ab')2 secondary antibody (Invitrogen A21237) was used to stain both the cells and QIFIKIT beads. The number of MSLN molecules on the surface was quantified using the QIFIKIT antigen standard curve.

Supplemental Figure 1

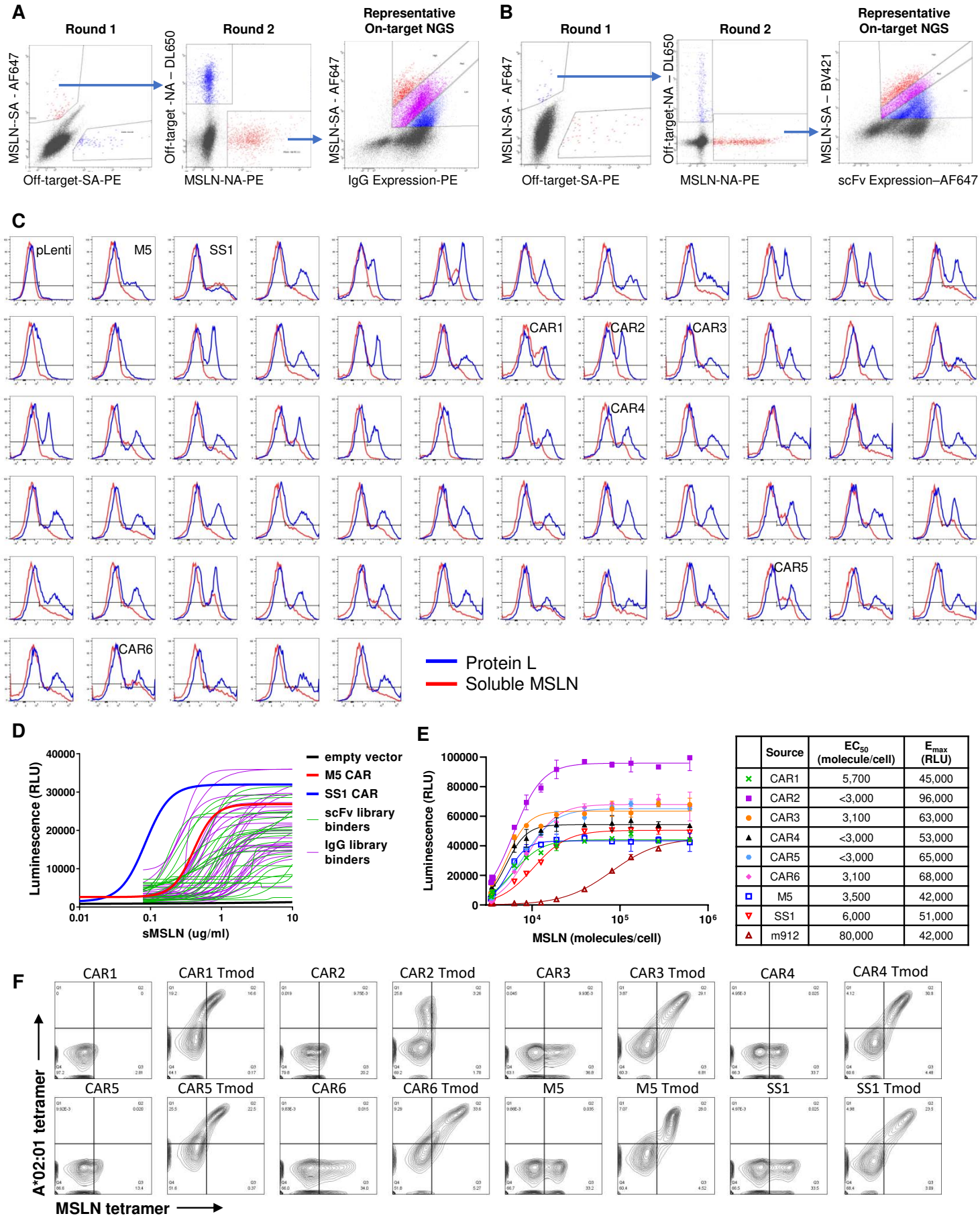

	Source	EC_{50} (molecule/cell)	E_{max} (RLU)
×	CAR1	5,700	45,000
■	CAR2	<3,000	96,000
●	CAR3	3,100	63,000
▲	CAR4	<3,000	53,000
●	CAR5	<3,000	65,000
◆	CAR6	3,100	68,000
□	M5	3,500	42,000
▽	SS1	6,000	51,000
△	m912	80,000	42,000

Supplemental Figure 1. Isolation and characterization of selective MSLN binders. To identify potent, selective MSLN-directed ligand-binding domains (LBDs) that function in CARs, two mammalian surface display libraries encoding either IgG antibodies (mAbs) or single-chain variable fragments (scFvs) were screened. (A) Enrichment of IgG library. (B) Enrichment of scFv library. PE, phycoerythrin; NA, neutravidin; SA, streptavidin. “On-target NGS” corresponds to the cell populations that were collected and subjected to DNA sequencing to determine enrichment of individual idiotypes. (C) After library enrichment, 62 individual LBDs were selected, converted to Gen3 scFv CARs and characterized. Jurkat cells were transiently transfected with CAR constructs and stained with Protein L (blue) or monomeric soluble MSLN (red). Benchmark and CAR1-6 expression histograms are labeled. (D) Functional response to surface-bound recombinant human MSLN (Acro Bio) was assessed in solid-state Jurkat cell assays (Hamburger et. al., *Mol Immunol* 2020). Most resulted in some response. (E) Sensitivity of MSLN CARs vs. benchmark CARs (M5, SS1 and m912) in a MSLN mRNA titration assay with HEK293T target cells using transfected Jurkat cells. Flow cytometry and QIFIKIT methodology were used to convert between mRNA amount and absolute MSLN molecules/cell. All constructs used Gen3 CARs, except for Gen2 SS1. For CARs with sensitivities below the limit of detection of the assay, EC_{50} was reported as <3K MSLN molecules/cell. Maximum signal (E_{max}) for each construct was also noted (n = 1-4 independent repeat experiments). (F) Jurkat cells transiently transfected with CAR +/- blocker constructs used in Figure 1C were stained with MSLN tetramer and A*02 tetramer to assess expression levels of activator and blocker receptors, respectively.

Supplemental Figure 2

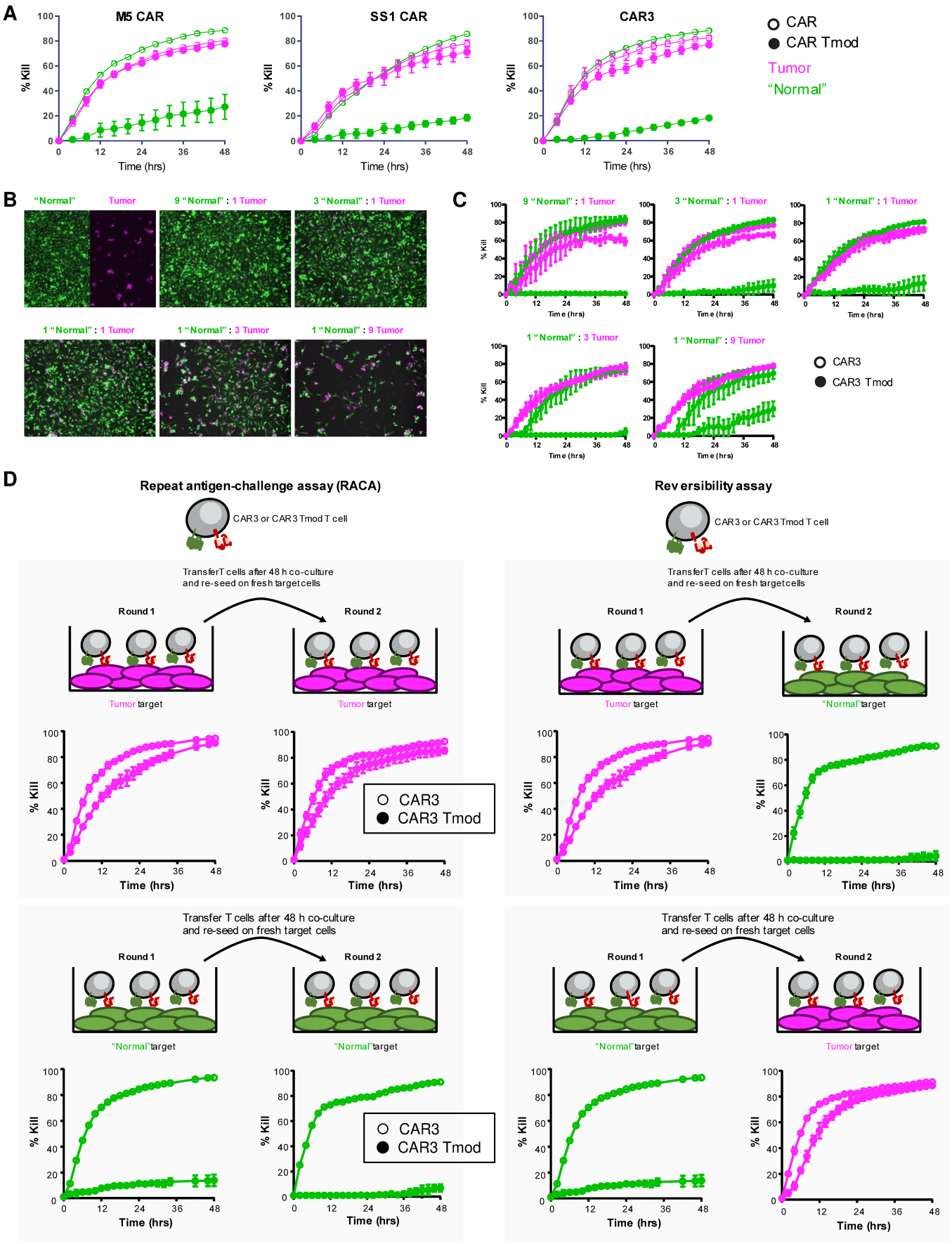

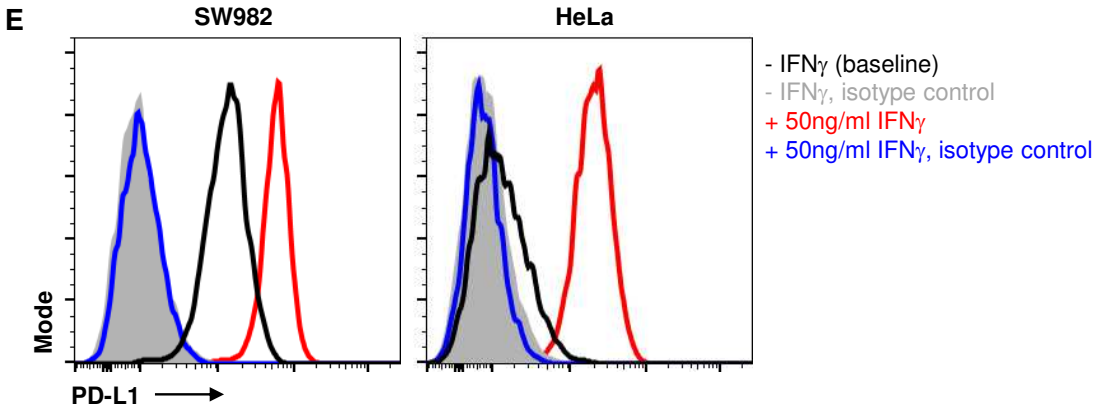

Supplemental Figure 2. MSLN CAR3 Tmod cells show robust and selective killing in mixed tumor/"normal" cell cultures and are unaffected by soluble MSLN (sMSLN). (A) Comparison of lead CAR3 activator paired with A*02 blocker to benchmark CARs in cytotoxicity assays. SS1 CAR is Gen2. Primary T cells transduced with various CARs +/- A*02 blocker using 2 separate lentiviral vectors were cultured with endogenous MSLN(+) HeLa cells to assess cytotoxicity. Tmod constructs showed selective killing in the context of all CARs and efficient blocking in the presence of A*02 antigen on "normal" target cells. Killing in the absence of MSLN was consistently low for all CARs (not shown). E:T = 0.6:1. (B) MSLN CAR3 Tmod cells selectively kill RFP(+) tumor cells and spare GFP(+) "normal cells" in mixed tumor/"normal" cell cultures. Images are representative of 48 h co-cultures at various "normal":tumor (N:T) ratios. Selective killing of tumor cells was observed even in the presence of high numbers of "normal" cells, while bystander killing of "normal" cells was only observed when significant killing of neighboring tumor cells occurred (i.e., low N:T). (C) Cytotoxicity of CAR3 (open circles) and CAR3 Tmod (closed circles) in mixed "normal" and tumor co-cultures with N:T ranging from 9:1 to 1:9; E:T = 0.6:1. (D) Schematic of repeat-antigen challenge assay (RACA) and reversibility assay shown in figure 4C. CAR3 (open circles) or CAR3 Tmod (closed circles) transduced primary T cells were co-cultured with either tumor or "normal" target cells for 48 h. T cells were then collected, depleted of dead or nonadherent target cells, and re-seeded onto fresh tumor or "normal" target cells for an additional 48 h. E:T = 1.2:1. While CAR3 T cells kill both "normal" (green open circles) and tumor (magenta open circles) cells in both rounds of the two assays, CAR3 Tmod selectively kill only tumor cells (magenta closed circles) and spare "normal" cells (green closed circles). (E) Baseline and IFNγ treated SW982 and HeLa target cell lines display variable levels of surface PD-L1.

Supplemental Figure 3

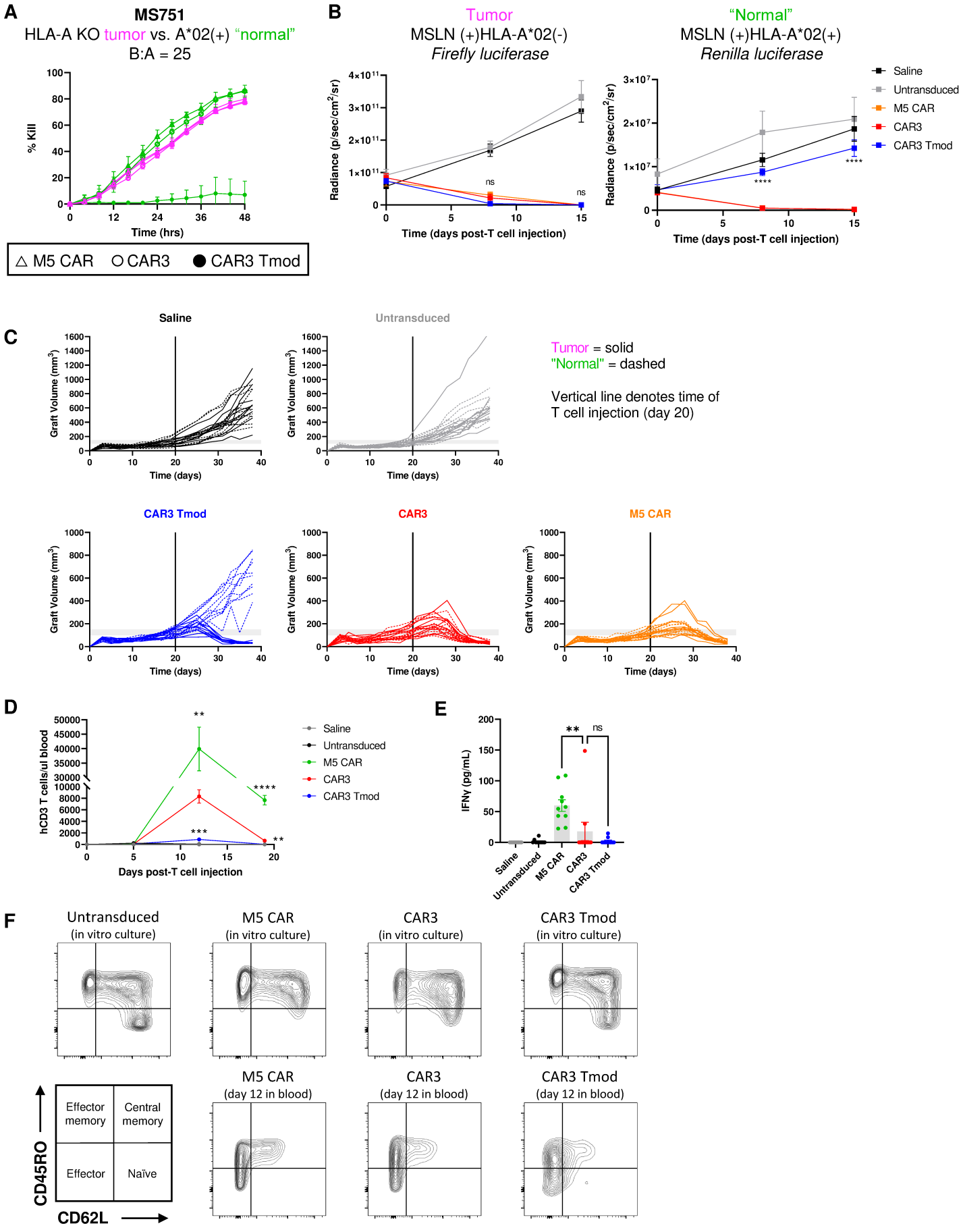

Supplemental Figure 3. Additional characterization of MSLN CAR3 Tmod tumor killing in xenograft model. (A) Primary T cells transduced with MSLN CARs or CAR3 Tmod were co-cultured with either HLA-A KO tumor or A*02-transgenic “normal” MS751 target cells in vitro. MSLN CAR3 Tmod displayed selective killing of tumor cells and blocked killing of “normal” cells in the presence of A*02 antigen. M5 CAR is Gen2; E:T = 1.4:1. (B) Bioluminescence imaging quantification of “normal” and tumor cells post-T cell injection for all groups. Two-way Anova with a multiple comparisons test was used to calculate differences between CAR3 and CAR3 Tmod at each timepoint. (C) Individual mouse xenograft growth curves for data shown in figure 5C. (D) T cell expansion in the peripheral blood shows significantly less CAR3 Tmod expansion compared to CAR3 T cells. (E) Serum IFNγ levels day 12 post-T cell injection. One-way Anova was used to calculate differences. (F) Representative phenotypic analysis of benchmark M5 CAR, CAR3, and CAR3 Tmod cells either in a parallel culture for 12 days (~4 weeks total culture time) maintained with constant IL2 or in peripheral blood 12 days post-T cell injection. Data in B-F include n = 10 animals per group.

Supplemental Figure 4

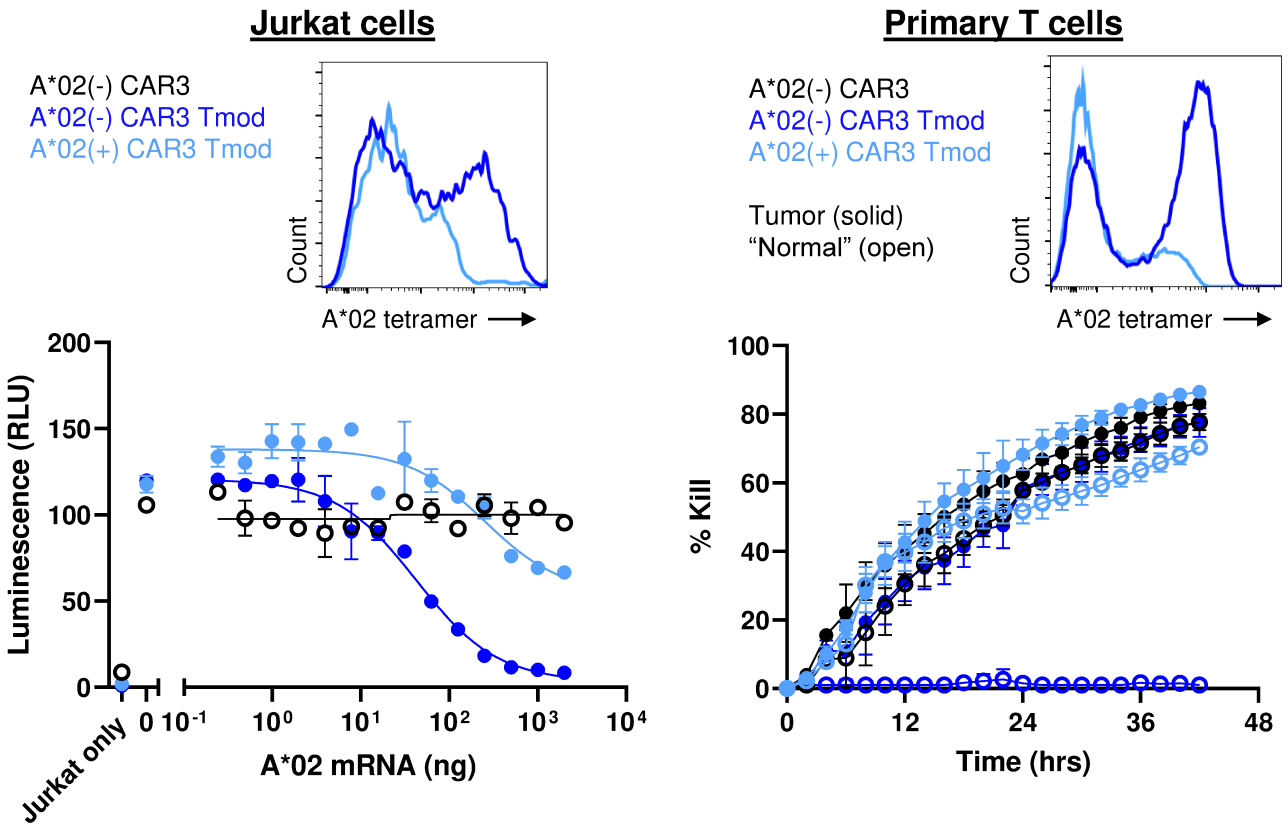

Supplemental Figure 4. Cis-binding of A*02 blocker in A*02(+) T cells abrogates function. Binding of the blocker in HLA-A*02(+) Jurkat cells and primary T cells by HLA-A*02 tetramer was significantly reduced due to cis-binding of autologous A*02. Reduced binding (due to reduced availability of the blocker) correlated with reduced blocker activity.

Supplemental Figure 5

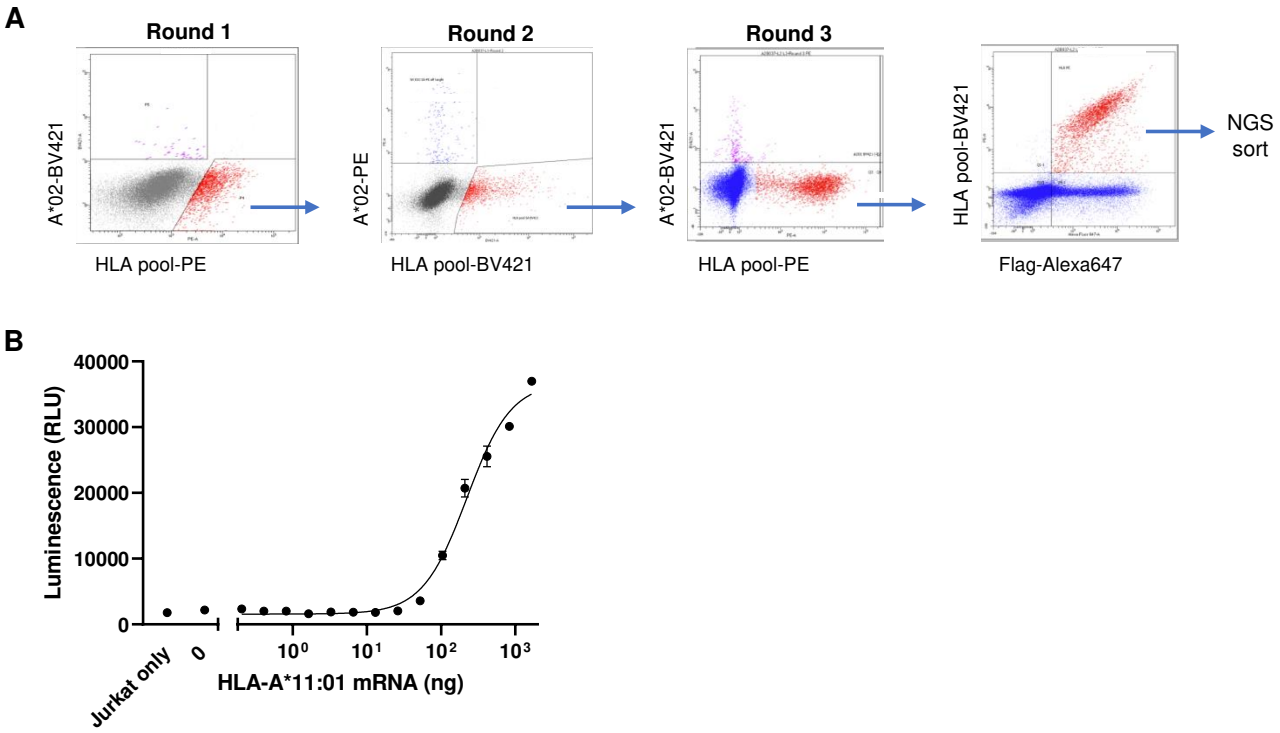

Supplemental Figure 5. Isolation and functional assessment of lead A*11 binder. (A) Enrichment of anti-A*11 binders through multiple rounds of cell sorting from an scFv library. PE, phycoerythrin. (B) Lead binder A*11 CAR4 expressed in Jurkat cells demonstrated functional activity in an A*11 mRNA titration assay using HeLa target cells.